Off-Resonance Angiography: A New Method to Depict Vessels—Phantom and Rabbit Studies[1]

Grigorios Korosoglou, MD[2]
Saurabh Shah, MS[3]
Evert-Jan Vonken, MD
Wesley D. Gilson, PhD
Michael Schär, PhD[4]
Lijun Tang, MD
Dara L. Kraitchman, VMD, PhD
Raymond C. Boston, PhD
David E. Sosnovik, MD
Robert G. Weiss, MD
Ralph Weissleder, MD, PhD
Matthias Stuber, PhD

Purpose: To evaluate the utility of inversion recovery with on-resonant water suppression (IRON) in combination with injection of the long-circulating monocrystalline iron oxide nanoparticle (MION)-47 for contrast material–enhanced magnetic resonance (MR) angiography.

Materials and Methods: Experiments were approved by the institutional animal care committee. Eleven rabbits were imaged at baseline before injection of a contrast agent and then serially 5–30 minutes, 2 hours, 1 day, and 3 days after a single intravenous bolus injection of 80 μmol of MION-47 per kilogram of body weight ($n = 6$) or 250 μmol/kg MION-47 ($n = 5$). Conventional T1-weighted MR angiography and IRON MR angiography were performed on a clinical 3.0-T imager. Signal-to-noise and contrast-to-noise ratios were measured in the aorta of rabbits in vivo. Venous blood was obtained from the rabbits before and after MION-47 injection for use in phantom studies.

Results: In vitro blood that contained MION-47 appeared signal attenuated on T1-weighted angiograms, while characteristic signal-enhanced dipolar fields were observed on IRON angiograms. In vivo, the vessel lumen was signal attenuated on T1-weighted MR angiograms after MION-47 injection, while IRON supported high intravascular contrast by simultaneously providing positive signal within the vessels and suppressing background tissue (mean contrast-to-noise ratio, 61.9 ± 12.4 [standard deviation] after injection vs 1.1 ± 0.4 at baseline, $P < .001$). Contrast-to-noise ratio was higher on IRON MR angiograms than on conventional T1-weighted MR angiograms (9.0 ± 2.5, $P < .001$ vs IRON MR angiography) and persisted up to 24 hours after MION-47 injection (76.2 ± 15.9, $P < .001$ vs baseline).

Conclusion: IRON MR angiography in conjunction with superparamagnetic nanoparticle administration provides high intravascular contrast over a long time and without the need for image subtraction.

Supplemental material: *http://radiology.rsnajnls.org/cgi/content/full/2491071706/DC1*

[1] From the Russell H. Morgan Department of Radiology and Radiological Science (G.K., S.S., E.J.V., W.D.G., M. Schär, L.T., D.L.K., R.G.W., M. Stuber) and Department of Medicine, Division of Cardiology (R.G.W.), Johns Hopkins University School of Medicine, 600 N Wolfe St, Park Bldg, Room 338, Baltimore, MD 21287; School of Veterinary Medicine, University of Pennsylvania, Kennett Square, Pa (R.C.B.); and Center for Molecular Imaging Research, Massachusetts General Hospital, Harvard Medical School, Boston, Mass (D.E.S., R.W.). Received September 26, 2007; revision requested January 10, 2008; revision received February 26; accepted April 7; final version accepted April 17. Supported by NIH grants 1 K08 EB004922-01, R01 HL084186, R01 HL61912, and R24 CA92782, as well as by the Donald W. Reynolds Foundation. **Address correspondence to** M. Stuber (e-mail: *mstuber@mri.jhu.edu*).

Current addresses:
[2] University of Heidelberg, Department of Cardiology, Heidelberg, Germany.
[3] Siemens Medical Solutions, Chicago, Ill.
[4] Philips Medical Systems, Cleveland, Ohio.

Radiology

Contrast material–enhanced magnetic resonance (MR) angiography is an imaging technique with a multitude of clinical applications (1–4). Currently, contrast-enhanced MR angiographic techniques are most commonly based on T1 shortening of blood caused by MR angiographic contrast agents (5,6). However, the short intravascular half-life of common low-molecular-weight gadolinium chelates limits the imaging time window and, therefore, the spatial resolution of contrast-enhanced MR angiography (5–7). For this reason, newer contrast agents, including gadolinium-based macromolecular contrast media and superparamagnetic nanoparticles, have been developed (7–13). These intravascular contrast agents remain in the vascular space for a prolonged time period, thereby permitting acquisition of high-spatial-resolution MR angiograms (7–13). The majority of MR angiographic approaches use intravascular agents to exploit the T1 shortening characteristics of contrast agents to achieve intravascular enhancement. However, undesirable signal from the surrounding tissue because of T1 recovery remains with these approaches; therefore, methods that support further improvement in blood-to-tissue contrast may represent a useful alternative.

Off-resonance imaging techniques were reported to create positive contrast in areas of superparamagnetic contrast materials (14–17). Inversion recovery with on-resonant water suppression (IRON) is a new off-resonance technique used to generate positive signal from superparamagnetic nanoparticles (18). In contrast to other off-resonance imaging techniques that use the frequency-selective excitation of off-resonance protons (17), the concept of IRON comprises the use of a spectrally selective saturation prepulse that suppresses the signal originating from on-resonant protons (Appendix E1, *http://radiology.rsnajnls.org/cgi/content/full/2491071706/DC1*). This prepulse is then followed by a conventional imaging sequence with on-resonant broadband radiofrequency excitation pulses. The saturation pulse does not affect off-resonant protons in areas of superparamagnetic nanoparticles; thus, signal enhancement adjacent to these particles can be generated while simultaneously the on-resonant background appears signal attenuated. The purpose of our study was to evaluate the utility of IRON in combination with injection of the long-circulating monocrystalline iron oxide nanoparticle (MION)-47 for contrast-enhanced MR angiography.

Advances in Knowledge

- Inversion recovery with on-resonant water suppression (IRON) MR angiography performed in conjunction with administration of superparamagnetic nanoparticles provides a new mechanism with which to generate contrast for MR angiography on a clinical 3.0-T imager.
- IRON MR angiography provides strong intravascular contrast within the vessel lumen over a long time and simultaneously suppresses background signal, without the need for image subtraction.

Implications for Patient Care

- Because of the high contrast-to-noise ratio and the long half-life of the contrast agent in the blood pool, IRON MR angiography supports excellent vessel conspicuity and high-spatial-resolution vascular imaging.
- IRON MR angiography may be useful in patient care for identification of luminal narrowing in small-diameter vessels and for evaluation of atherosclerosis progression.

Materials and Methods

One author (M. Stuber) is compensated as a consultant for Philips Medical Systems (Best, the Netherlands) (ie, the manufacturer of the equipment used in our study), one author (M. Schär) is an employee of Philips Medical Systems, and one author (S.S.) is an employee of Siemens Medical Solutions. The authors who are not consultants for or employees of Philips Medical Systems or Siemens Medical Solutions had full control of the inclusion of any data or information that might have presented a conflict of interest for these authors.

Animals

The studies were approved by the animal care and use committee of Johns Hopkins University. Experiments were conducted in 11 male rabbits (2.5–3.2 kg) that were sedated with acepromazine (1 mg per kilogram of body weight) and ketamine (40 mg/kg) administered intramuscularly. General anesthesia was maintained with thiopental administered intravenously. For phantom studies, venous blood was obtained from the ear vein before and 30 minutes and 1 day after MION-47 injection.

Phantoms

The 1% agar gel (Sigma-Aldrich, St Louis, Mo) was prepared in 150-mm-diameter tissue culture dishes (BD Biosciences, San Jose, Calif). Heparinized venous rab-

Published online before print
10.1148/radiol.2491071706

Radiology 2008; 249:501–509

Abbreviations:
CNR = contrast-to-noise ratio
IRON = inversion recovery with on-resonant water suppression
MION = monocrystalline iron oxide nanoparticle
ROI = region of interest

Author contributions:
Guarantors of integrity of entire study, G.K., M. Stuber; study concepts/study design or data acquisition or data analysis/interpretation, all authors; manuscript drafting or manuscript revision for important intellectual content, all authors; manuscript final version approval, all authors; literature research, W.D.G., D.L.K., D.E.S., M. Stuber; experimental studies, G.K., S.S., E.J.V., W.D.G., M. Schär, L.T., R.G.W., M. Stuber; statistical analysis, G.K., S.S., D.L.K., R.C.B.; and manuscript editing, G.K., S.S., E.J.V., W.D.G., M. Schär, D.L.K., R.C.B., D.E.S., R.G.W., R.W., M. Stuber

Funding:
This research was funded by the National Institutes of Health (grants 1 K08 EB004922-01, R01 HL084186, R01 HL61912, R24 CA92782).

See Materials and Methods for pertinent disclosures.

See also Science to Practice in this issue.

bit blood was transferred in 1.0-mL Eppendorf tubes that were embedded in the agar gel. A probe containing mineral oil was included to test the efficacy of fat suppression.

Contrast Agent

One of the authors (R.W.) synthesized MION-47 at the Center for Molecular Imaging Research (Massachusetts General Hospital, Harvard Medical School). MION-47 is a stable nanoparticle that shortens the longitudinal (T1) and transverse (T2) relaxation times (19–21). MION-47 consists of a monocrystalline magnetite-like single-crystal core. The average size of the nanoparticles used in our study was 27.5 nm ± 6.8 (standard deviation), the R1 and R2 relaxivity rates were 25.5 mM/sec and 53.7 mM/sec respectively, and the plasma half-life was 11.4 hours ± 0.6 in mice (20). In our study, a single bolus injection of 80 μmol/kg MION-47 was administrated in six rabbits, whereas a single bolus injection of 250 μmol/kg MION-47 was administered in five rabbits.

MR Imaging

MR imaging was performed with a clinical 3.0-T whole-body MR unit (Achieva; Philips Medical Systems). Phantoms were imaged with a six-element cardiac phased-array receiver coil used in humans. Imaging of rabbits was performed serially before single bolus injection of contrast material and 5–30 minutes, 2 hours, 1 day, and 3 days after contrast agent injection (Fig 1) with use of a four-element carotid receiver coil used in humans (Pathway MRI, Seattle, Wash). The same imaging parameters were used for in vitro and in vivo imaging. For all imaging procedures, higher-order shimming was used (22).

Quantitative T1 measurements.—A Look-Locker sequence (23) was applied in vivo to determine the T1 values of arterial blood. The imaging parameters for the Look-Locker sequence were as follows: repetition time msec/echo time msec, 3.8/2.3; 6° flip angle; 260 × 156-mm field of view; bandwidth, 189 Hz/pixel; and 304 × 174 image matrix resulting in a 0.9 × 0.9 × 9-mm acquired voxel size. The examination yielded a time series of 50 images, on which signal intensities followed the T1-mediated regrowth of longitudinal magnetization after a 180° inversion pulse. In between these inversion pulses, a recovery period (Td) of 2.5–10.0 seconds (more than five times the expected T1 value of blood) was used.

With this approach, the time from magnetization inversion until inversion recovery was measured to the time point of signal nulling (T_{Inv}), and T1 values were numerically calculated with Excel software (Microsoft, Redmond, Wash) and the following equation (24): $T_{Inv} = T1 \cdot \ln[2/(1 + e^{-Td/T1})]$.

Conventional T1-weighted MR imaging.—For T1-weighted MR imaging, three-dimensional gradient-echo images were obtained by using the following parameters: 25/2.7, 20° flip angle, 200 × 100-mm field of view, 217 Hz/pixel bandwidth, and 400 × 200 image matrix. For in vivo imaging, a 5.0-cm-thick three-dimensional volume was imaged with 50 z-encoding steps (0.5 × 0.5 × 1-mm acquired voxel size). Imaging time was 3 minutes.

IRON imaging.—For off-resonance imaging, an on-resonant frequency-selective IRON suppression prepulse with a 100-Hz bandwidth and a 100° flip angle was used to suppress the signal originating from on-resonant protons (18) (Appendix E1, *http://radiology.rsnajnls.org/cgi/content/full/2491071706/DC1*). Another frequency-selective prepulse preceding the IRON prepulse with a −480-Hz frequency offset, a 500-Hz bandwidth, and a 105° flip angle was used for fat saturation. Typical parameters for the three-dimensional segmented k-space gradient-echo imaging sequence that followed the IRON prepulse were as follows: 3.9/1.5, 19 broadband on-resonant radiofrequency excitations per k-space segment with a constant 15° flip angle, 74-msec acquisition window, 140 × 112-mm field of view, partial echo, 642 Hz/pixel bandwidth, and 288 × 220 image matrix. For in vivo imaging, a 5.0-cm-thick three-dimensional volume was examined with 25 z-encoding steps (0.49 × 0.51 × 2-mm acquired voxel size). Imaging time was 3 minutes. T1-weighted and IRON MR angiograms were obtained at baseline and 5–30 minutes, 2 hours, 1 day, and 3 days after contrast agent injection.

Source of positive signal on IRON images.—In six rabbits that received 80 μmol/kg MION-47, two series of pulses were applied 5–30 minutes after injection: One series had variable bandwidth and incremental durations (3, 5, 10, 15, 20, 30, 40, and 50 msec), whereas the other series had increasing time delays (5.5, 6.5, 9.0, 11.5, 14.0, 19.0, 24.0, and 29.0 msec) and a constant duration of 3 msec. The signal-to-noise ratio and contrast-to-noise ratio (CNR) were subsequently quantified on all of the resultant images (Appendix E1, *http://radiology.rsnajnls.org/cgi/content/full/2491071706/DC1*).

Image analysis.—Quantitative analysis of in vivo MR angiograms was performed with the SoapBubble Tool (release 5.0 for Pride V5; Philips Medical Systems) (25,26). An author (G.K., 6 years of experience in cardiovascular imaging) quantified the signal-to-noise ratio and CNR by using original nonreformatted magnitude images, without use of sensitivity encoding or constant level appearance, as described previously (25) (Appendix E1, *http://radiology.rsnajnls.org/cgi/content/full/2491071706/DC1*). Regions of interest (ROIs) were placed manually in the abdominal aorta and in

Figure 1

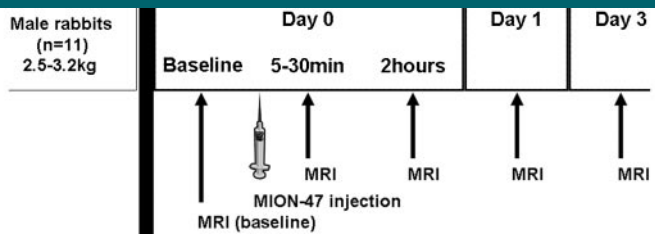

Figure 1: Flow diagram of the animal studies.

the inferior caval vein at the level of the left renal artery to measure the mean blood signal intensity (SI_b). Signal intensity of adjacent muscle (SI_m) was measured by choosing an ROI similar in size to ROIs in the abdominal aorta and in the inferior caval vein adjacent to the aorta. ROIs were also placed in the air outside the rabbit. The standard deviation of the signal in this ROI was used as a measure of background noise (σ). The signal-to-noise ratio (SNR) was calculated with the following equation: $SNR = SI_b/\sigma$, and CNR was calculated with the following equation: $CNR = (SI_b - SI_m)/\sigma$.

Care was taken to standardize ROI size and placement for better comparison between image sets. The mean size of ROIs placed in vessels was 0.30 $cm^2 \pm 0.04$, the mean size of those placed in adjacent muscle was 0.33 $cm^2 \pm 0.04$, and the mean size of those placed in the background was 7.3 $cm^2 \pm 0.9$.

Statistical Analysis

Data are presented as means ± standard deviations. On the basis of the expected increase in CNR after administration of MION-47, we estimated that five or six animals in each group would be sufficient to yield a statistical power of more than 90%, with α of .05 considered to indicate significant differences in intravascular contrast enhancement. To correct for serial correlation among measurements, differences in T1 values and differences in CNRs between different time points and between IRON and T1-weighted MR angiography were compared with a cross-sectional time series regression model by using a generalized least-squares estimator with a random-effects model for between-regression estimations. Furthermore, to correct for the lack of independence in our data because of repeated observations in rabbits, a clustered regression approach was used to compare differences in signal-to-noise ratio and CNR between IRON images acquired with the same time delay and different durations of the IRON prepulse. Differences in CNR between the aorta and the caval vein were evaluated with a paired *t* test. $P < .05$ was considered to indicate a significant difference. Calculations were performed with statistical software (Stata, version 9.2; Stata, College Station, Tex).

Figure 2

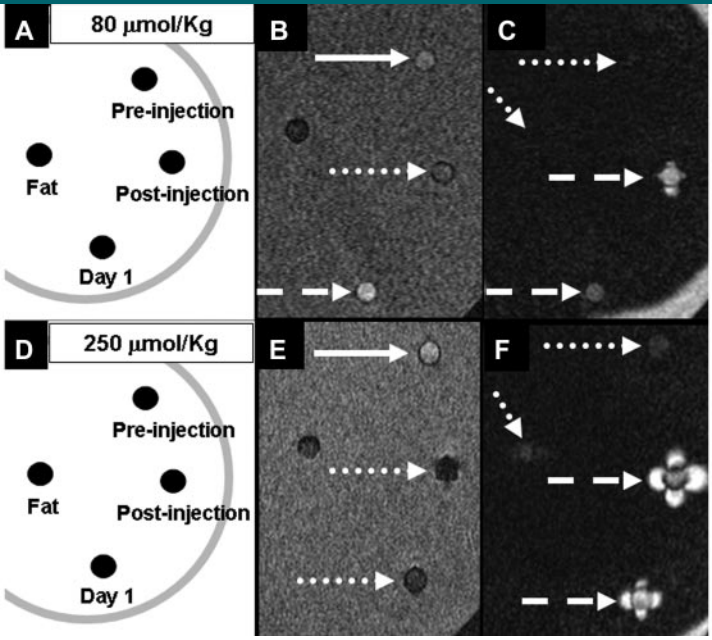

Figure 2: Phantoms that included blood collected from rabbits before and after injection of, *A–C*, 80 μmol/kg MION-47 and, *D–F*, 250 μmol/kg MION-47 were imaged with T1-weighted (*B* and *E*) and IRON (*C* and *F*) MR angiography. On coronal T1-weighted angiograms (25.0/2.7, 20° flip angle), blood samples with high concentrations of MION-47 were hypointense (dotted arrows in *B* and *E*) compared with those obtained at baseline (solid arrows in *B* and *E*), while blood collected 1 day after injection of 80 μmol/kg MION-47 with a relatively low concentration had increased signal (dashed arrow in *B*). On IRON MR angiograms (3.9/1.5, 15° flip angle), background and fat (dotted arrows in *C* and *F*) were strongly suppressed, while blood containing MION-47 (dashed arrows in *C* and *F*) showed signal-enhanced characteristic dipolar structures.

Results

In Vitro Blood Studies

Blood collected 30 minutes after injection of 80 μmol/kg MION-47 appeared signal attenuated on conventional T1-weighted images, whereas blood collected 1 day after injection of 80 μmol/kg MION-47 had increased signal (Fig 2, *B*). Blood appeared signal attenuated up to 24 hours after injection of 250 μmol/kg MION-47 (Fig 2, *E*). With use of IRON MR angiography, agar gel, blood collected before MION-47 injection, and fat were signal attenuated, whereas blood collected after MION-47 injection showed highly signal-enhanced characteristic dipolar fields around the test tubes (Figs 2, *C*, *F*).

In Vivo T1-weighted MR Angiography

Both the thoracic aorta and the abdominal aorta were signal-attenuated after MION-47 injection on conventional T1-weighted MR angiograms when compared with baseline images (Fig 3). The signal in the vessel lumen returned 1 day after injection and approached that seen at baseline 3 days after injection (Fig 3). Quantitative T1 measurements revealed concentration-dependent T1 shortening of blood in vivo, which was related to the dose of MION-47 injected and inversely related to the interval between injection and imaging (Table). For both of the MION-47 doses (80 μmol/kg and 250 μmol/kg), there was significant T1 shortening directly after contrast agent injection and 1 day after

Figure 3

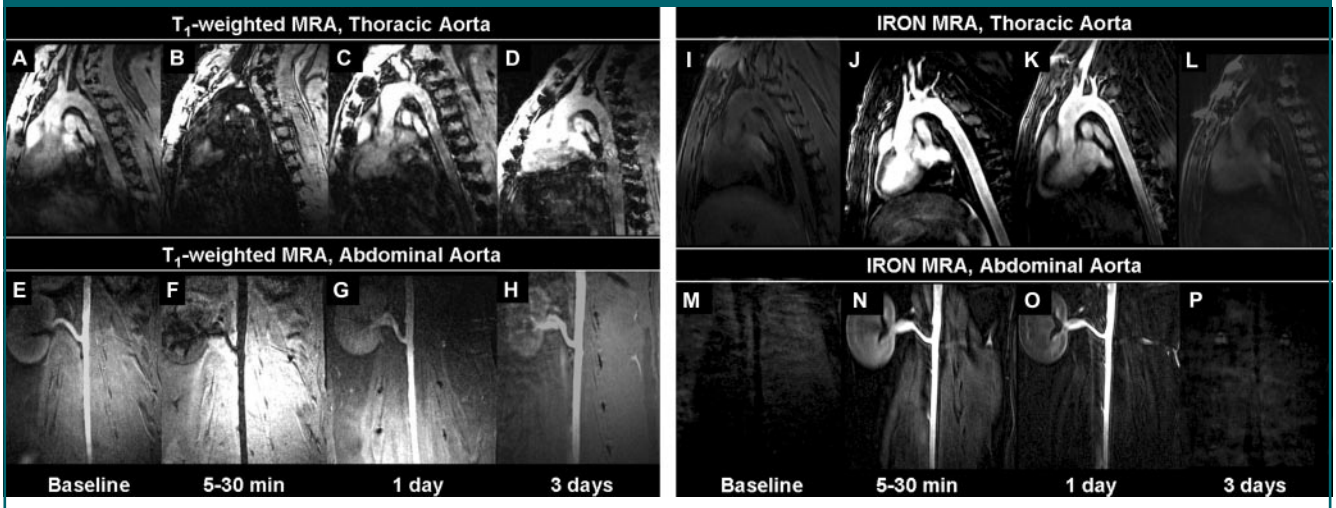

Figure 3: On sagittal conventional T1-weighted MR angiograms (25/2.7, 20° flip angle), the aorta of the rabbits was signal attenuated 5–30 minutes after MION-47 injection (*B* and *F*) when compared with that at baseline (*A* and *E*). Intravascular signal returned 1 day after injection (*C* and *G*) and approached that at baseline 3 days after injection (*D* and *H*). On sagittal IRON MR angiograms (3.9/1.5, 15° flip angle), fat, muscle, and blood were homogeneously suppressed at baseline (*I* and *M*). After injection, the aorta was strongly signal enhanced, and the surrounding tissue was signal attenuated, supporting high intravascular contrast (*J* and *N*), which persisted up to 24 hours after injection (*K* and *O*) and approached the baseline level 3 days after injection (*L* and *P*).

contrast agent injection when compared with T1 at baseline ($P < .001$). In addition, there was a more intense decrease in T1 with the high dose than with the low dose ($P < .002$). This was most notable 1 day after injection.

In Vivo IRON MR Angiography

With use of IRON MR angiography, the lumen of the thoracic aorta and that of the abdominal aorta was strongly enhanced after MION-47 injection. Simultaneously, background tissues, including fat and muscle, appeared strongly signal attenuated, and image subtraction was not needed. This finding supported high intravascular contrast, which persisted up to 24 hours after contrast material injection and approached the baseline level 3 days after injection (Fig 3).

Quantitative Analysis of T1-weighted MR Angiography and IRON MR Angiography

For injection of 80 μmol/kg MION-47, CNR decreased on T1-weighted MR angiograms 5–30 minutes and 2 hours after injection ($P < .001$ vs baseline for both), CNR increased 1 day after injection ($P < .001$ vs baseline), and CNR returned to the baseline value 3 days after injection (Fig 4, *A*). With use of IRON, CNR increased markedly after MION-47 injection ($P < .001$ vs baseline) and was similarly high both 2 hours and 1 day after injection ($P < .001$ vs baseline for both). After administration of 250 μmol/kg MION-47 ($n = 5$), CNR was negative on T1-weighted MR angiograms obtained 5–30 minutes after injection and 2 hours after injection ($P < .001$ vs baseline for both) and returned to the baseline value 3 days after injection. With use of IRON, a striking increase in CNR was noticed 5–30 minutes after injection of 250 μmol/kg MION-47 (61.9 ± 12.4 after injection vs 1.1 ± 0.4 at baseline, $P < .001$). CNR remained high 2 hours and 1 day after injection ($P < .001$ vs baseline for both) (Fig 4, *B*). There was no significant difference in the pattern of CNR changes between the low and high contrast agent doses on IRON images. Furthermore, the CNR on IRON MR angiograms was markedly higher than that on conventional T1-weighted MR angiograms (9.0 ± 2.5, $P < .001$ vs

T1 Values of Arterial Blood in the Abdominal Aorta of Rabbits at Baseline and after MION-47 Injection

Time Point	T1 Value in Rabbits That Received an 80 μmol/kg Dose of MION-47 (msec)	T1 Value in Rabbits That Received a 250 μmol/kg Dose of MION-47 (msec)
Baseline	1643 ± 69	1657 ± 61
Within 2 hours after injection	109 ± 11*	37 ± 6*†
1 day after injection	375 ± 125‡	125 ± 32†‡
3 days after injection	1685 ± 84	1633 ± 79

Note.—Data are means ± standard deviations.

* $P < .001$ within 2 hours after injection of MION-47 versus baseline.

† $P < .002$ within 2 hours and 1 day after injection of 80 μmol/kg versus 250 μmol/kg MION-47.

‡ $P < .001$ 1 day after injection of MION-47 versus baseline.

IRON MR angiography) and persisted up to 24 hours after MION-47 injection (76.2 ± 15.9, $P < .001$ vs baseline). In addition, CNR in the caval vein on IRON MR angiograms was similar to that in the aorta after MION-47 injection (62.7 ± 13.9 vs 62.1 ± 11.4, respectively; $P \geq .05$).

Figure 4

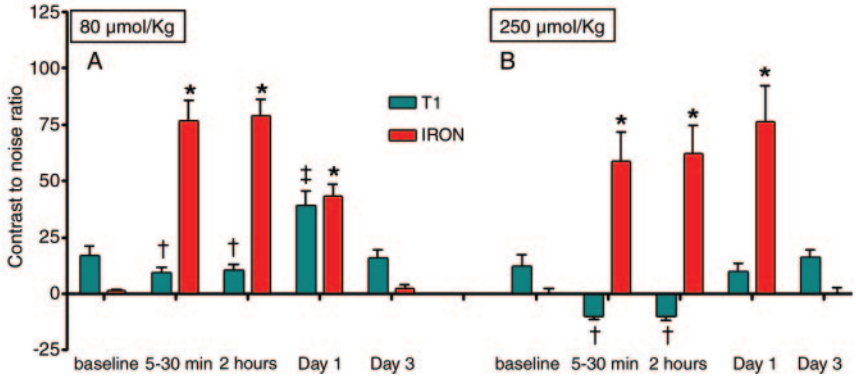

Figure 4: After injection of, *A,* 80 μmol/kg MION-47 ($n = 6$), and, *B,* 250 μmol/kg MION-47 ($n = 5$), CNR decreased on T1 weighted MR angiograms 5–30 minutes and 2 hours († indicates $P < .001$ vs baseline) after injection and returned to baseline 3 days ($P \geq .05$) after injection, while CNR significantly increased 1 day after injection of 80 μmol/kg (‡indicates $P < .001$ vs baseline). On IRON MR angiograms, CNR markedly increased after injection, remained high 2 hours and after 1 day after injection (∗ indicates $P < .001$ vs baseline for all), and returned to baseline 3 days after injection ($P \geq .05$). The CNR on IRON MR angiograms was markedly higher than that on conventional T1-weighted MR angiograms ($P < .001$).

Quantification of the Sources of Positive Signal on IRON MR Angiograms

By gradually increasing the duration of the IRON prepulse (Appendix E1, *http://radiology.rsnajnls.org/cgi/content/full/2491071706/DC1*), intravascular signal increased by a significantly ($P < .001$) higher degree than that obtained with an incremental delay between the IRON prepulse and the imaging part of the sequence (Figs 5, 6). For bandwidth of the IRON prepulse of 100 Hz (50-msec duration and 29-msec delay), CNR was 83.1. For the corresponding bandwidth of the IRON prepulse of 1667 Hz (3-msec duration with broadband suppression of on- and off-resonant protons and 29-msec delay), CNR was 34.6. Thus, 42% of intravascular contrast was attributable to T1 shortening (ie, $CNR_{T1rec}/CNR_{tot} = 34.6/83.1$), where CNR_{T1rec} is CNR for T1 recovery and CNR_{tot} is total CNR. The remaining 58% (ie, $[CNR_{tot} - CNR_{T1rec}]/$

Figure 5

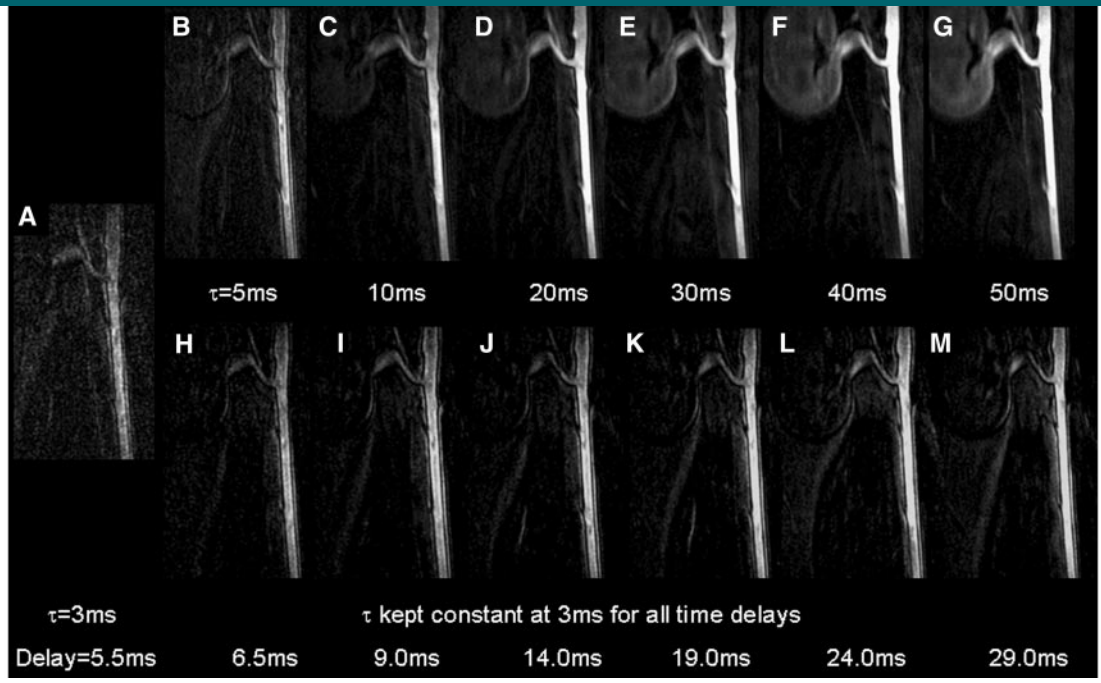

Figure 5: By increasing the duration of the IRON prepulse (τ), intravascular signal increased to a higher degree *(A–G)* when compared with that obtained with an incremental time delay between the IRON prepulse and the imaging part of the sequence *(H–M). ms* = milliseconds.

CNR_{tot} = 48.5/83.1) was attributed to off resonance.

Discussion

IRON MR angiography performed in conjunction with administration of superparamagnetic nanoparticles offers a new source of contrast enhancement for in vivo vascular imaging by providing a high signal from the blood pool and by simultaneously suppressing signal from background tissue. This leads to high contrast between the blood pool and the surrounding tissue, thereby supporting vessel conspicuity without the need for image subtraction. Because of these characteristics and in concert with the long half-life of the contrast agent in the blood pool, IRON MR angiography seems well suited for three-dimensional imaging, which inherently necessitates prolonged examination times. IRON MR angiography may facilitate serial evaluations (ie, before and after interventions), thereby obviating the need for repeated contrast agent injections, and it may provide a useful adjunct or alternative to more conventional T1-weighted MR angiography methods for use in the identification and characterization of vascular disease. Because MION-47 is analogous to ferumoxtran, which has completed phase III clinical trials, the translation of these findings to the clinical realm appears promising (27,28).

Furthermore, in light of earlier work by Ruehm et al (29), this technique may have the potential to be used in a more comprehensive assessment of vascular disease because iron uptake by macrophages in the atherosclerotic vessel wall may lead to off-resonance signal enhancement once the agent has cleared the blood pool. Because the phagocytosis of superparamagnetic particles occurs gradually and reaches its maximum level several days after administration (29,30), intraluminal off-resonance signal is expected to be low at these later time points, thereby allowing for better definition of the vessel wall and for detection of positive signal in areas of macrophage-dense atherosclerotic plaque.

Figure 6

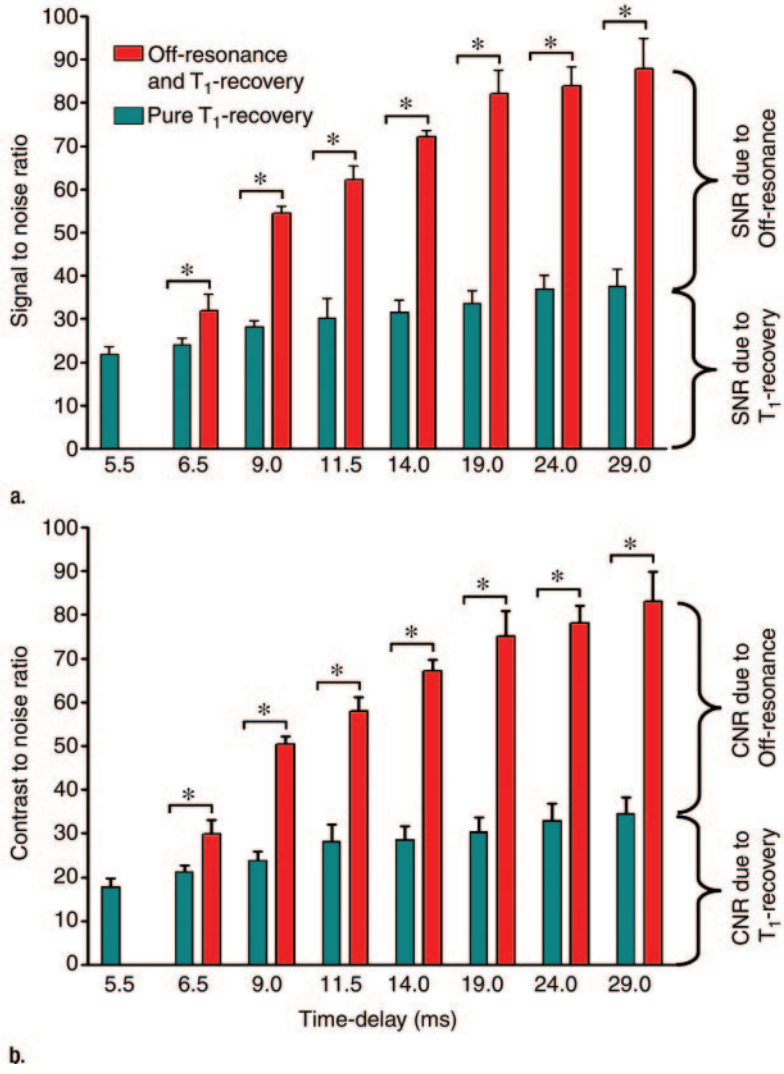

Figure 6: Increases in **(a)** signal-to-noise ratio and **(b)** CNR were significantly higher when the duration of the IRON prepulse was increased in comparison with increases observed with an incremental time delay (* indicates $P < .001$ with clustered regression analysis).

Our results show that the intravascular contrast provided by IRON MR angiography is significantly higher than that provided by conventional T1-weighted MR angiography after administration of a single bolus of MION-47. The spatial resolution, total imaging volume, and duration of IRON MR angiography and T1-weighted MR angiography were similar. Furthermore, the dual origin of positive signal on IRON images was characterized, and the relative contribution of each source of signal was quantified. Thus, with use of IRON MR angiography, approximately 58% of the contrast can be attributed to off resonance, and the remaining 42% can be attributed to T1 recovery. In fact, the combination of signal originating from off resonance and signal originating from T1 recovery results in a high CNR, which is sustainable for a long time.

Since signal enhancement was present in blood samples containing MION-47 in static phantoms and since similarly high CNR was measured in the caval vein of

rabbits after injection, inflow was not considered a major contributor to overall contrast. This may represent an advantage of IRON MR angiography techniques over flow-dependent MR angiography techniques, such as time-of-flight imaging, where diminished blood flow may result in low contrast formation within the vessels of interest (26,31).

Recently, an alternative MR angiography technique, off-resonance contrast angiography (ORCA), that is dependent on magnetic susceptibility effects after gadolinium chelate administration was introduced and used to generate in vivo images in human subjects (17). ORCA combines a frequency-selective excitation with a broadband presaturation pulse for background signal suppression. The signal enhancement obtained with this first implementation of ORCA is strongly dependent on vessel orientation (17). On in vivo IRON MR angiograms, both the descending aorta (oriented parallel with the main magnetic field) and the renal arteries (oriented perpendicular to the main magnetic field) were displayed with positive contrast. Similarly, in the ascending aorta and the aortic arch, no orientation-dependent signal attenuation was identified. This may be attributable to two effects: First, after injection of MION-47, both off resonance and a short T1 contribute to the signal in the blood pool (Appendix E1, *http://radiology.rsnajnls.org/cgi/content/full/2491071706/DC1*). Since the T1 contrast is not orientation dependent, a total signal void is not expected for any orientation of the vessels relative to the main magnetic field. Second, since the IRON technique inherently displays both positive and negative off resonance equally, the signal originating from off resonance is less dependent on orientation when compared with that generated with methods that attenuate larger parts of the frequency spectrum. However, these effects have to be investigated in more detail, and they will need to be characterized more rigorously. Simultaneously, a discrepancy between in vitro and in vivo images was observed in our study: Characteristic signal-enhanced dipole formations (artifactual structures) were present on in vitro IRON MR angiograms but not on in vivo images. Obvious differences in the dimensions (higher length-to-diameter ratio in blood vessels than in tubes), lower blood oxygenation levels in vitro versus in vivo, or clustering of the contrast agent in vitro may have contributed to the observed differences. Furthermore, while positive signal was found outside the test tube containing blood and 250 μmol/kg MION-47 in vitro, the area of positive signal was constrained to the test tube alone when 80 μmol/kg MION-47 was used. For this reason and because in vivo human applications will likely be performed at even lower doses, this effect may be reduced even further. Nevertheless, with high contrast agent doses and particularly with small vessels running perpendicular to the main magnetic field, signal enhancement from outside of the lumen blood pool is a concern and may adversely affect lumen diameter measurements and estimation of stenosis.

Our study had some limitations. The number of animals studied was relatively small. However, to our knowledge, we are the first to report use of this technique and to demonstrate its feasibility, both in vitro and in vivo. Despite the small number of animals studied, the magnitude of contrast enhancement was similar among animals, as evidenced by the relatively small standard deviation of CNR measurements. The MION-47 doses injected in rabbits were higher than the recommended clinical dose in humans (46 μmol/kg) (30). However, ferumoxtran, which is highly analogous to MION-47, has demonstrated a satisfactory safety profile in several animal (32) and clinical (27) studies. Furthermore, in our study, CNR remained high even 1 day after injection; therefore, it can be expected that lower doses of superparamagnetic nanoparticles may be adequate for steady-state MR angiography up to a few hours after injection. Furthermore, specific T2*-weighted imaging was not performed in our study; thus, the relative contribution of T2* effects on T1-weighted images and IRON images merits further investigation. Nevertheless, on a conventional MR angiogram, a signal void was observed in the aorta shortly after contrast agent administration (Fig 3, *B*); this finding may be related to T2* shortening consistent with the high concentration of the contrast agent.

In conclusion, IRON MR angiography generates positive signal in the presence of superparamagnetic nanoparticles in the blood pool. Hereby, off resonance is responsible for signal enhancement in the blood pool, while signal from on-resonant protons in the background is effectively suppressed. This leads to high contrast between the blood pool and the surrounding tissue, which surpasses that from more conventional T1-weighted MR angiography. Since the off-resonance effects persist until 1 day after contrast agent administration, this method effectively supports the use of high-spatial-resolution imaging, and repeat examinations with only one injection of the contrast agent may be feasible. This noninvasive technique has the potential to further improve the delineation of vascular anatomy, and it may possibly improve the identification of vascular disease.

Practical applications: IRON MR angiography performed in conjunction with administration of superparamagnetic nanoparticles results in strong intravascular enhancement that is sustainable over a long time. This technique may have the potential to be used for a more comprehensive assessment of vascular disease, since iron uptake by macrophages in the atherosclerotic vessel wall may also lead to off-resonance signal enhancement. Furthermore, this method may be useful for evaluation of small collateral vessels and the progress of arteriogenesis, as well as for monitoring angiogenesis suppression therapies in patients with cancer.

References

1. Prince MR, Narasimham DL, Stanley JC, et al. Breath-hold gadolinium-enhanced MR angiography of the abdominal aorta and its major branches. Radiology 1995;197:785–792.

2. Prince MR, Yucel EK, Kaufman JA, Harrison DC, Geller SC. Dynamic gadolinium-enhanced three-dimensional abdominal MR arteriography. J Magn Reson Imaging 1993;3:877–881.

3. Snidow JJ, Harris VJ, Trerotola SO, et al. Interpretations and treatment decisions based on MR angiography versus conventional arteriography in symptomatic lower extremity ischemia. J Vasc Interv Radiol 1995;6:595–603.

4. Tatli S, Lipton MJ, Davison BD, Skorstad RB, Yucel EK. From the RSNA refresher courses: MR imaging of aortic and peripheral vascular disease. RadioGraphics 2003; 23(Spec Issue):S59–S78.

5. Yucel EK. MR angiography for evaluation of abdominal aortic aneurysm: has the time come? Radiology 1994;192:321–323.

6. Prince MR. Gadolinium-enhanced MR aortography. Radiology 1994;191:155–164.

7. Grist TM. Future directions of magnetic resonance angiography. Invest Radiol 1998;33: 485–487.

8. Allkemper T, Heindel W, Kooijman H, Ebert W, Tombach B. Effect of field strengths on magnetic resonance angiography: comparison of an ultrasmall superparamagnetic iron oxide blood-pool contrast agent and gadopentetate dimeglumine in rabbits at 1.5 and 3.0 tesla. Invest Radiol 2006;41:97–104.

9. Clarke SE, Weinmann HJ, Dai E, Lucas AR, Rutt BK. Comparison of two blood pool contrast agents for 0.5-T MR angiography: experimental study in rabbits. Radiology 2000; 214:787–794.

10. Allkemper T, Bremer C, Matuszewski L, Ebert W, Reimer P. Contrast-enhanced blood-pool MR angiography with optimized iron oxides: effect of size and dose on vascular contrast enhancement in rabbits. Radiology 2002;223:432–438.

11. Frank H, Weissleder R, Brady TJ. Enhancement of MR angiography with iron oxide: preliminary studies in whole-blood phantom and in animals. AJR Am J Roentgenol 1994; 162:209–213.

12. Mayo-Smith WW, Saini S, Slater G, Kaufman JA, Sharma P, Hahn PF. MR contrast material for vascular enhancement: value of superparamagnetic iron oxide. AJR Am J Roentgenol 1996;166:73–77.

13. Wang SC, Wikstrom MG, White DL, et al. Evaluation of Gd-DTPA-labeled dextran as an intravascular MR contrast agent: imaging characteristics in normal rat tissues. Radiology 1990;175:483–488.

14. Bakker CJ, Seppenwoolde JH, Vincken KL. Dephased MRI. Magn Reson Med 2006;55: 92–97.

15. Seppenwoolde JH, Viergever MA, Bakker CJ. Passive tracking exploiting local signal conservation: the white marker phenomenon. Magn Reson Med 2003;50:784–790.

16. Cunningham CH, Arai T, Yang PC, McConnell MV, Pauly JM, Conolly SM. Positive contrast magnetic resonance imaging of cells labeled with magnetic nanoparticles. Magn Reson Med 2005;53:999–1005.

17. Edelman RR, Storey P, Dunkle E, et al. Gadolinium-enhanced off-resonance contrast angiography. Magn Reson Med 2007;57:475–484.

18. Stuber M, Gilson WD, Schar M, et al. Positive contrast visualization of iron oxide-labeled stem cells using inversion-recovery with ON-resonant water suppression (IRON). Magn Reson Med 2007;58:1072–1077.

19. Shen T, Weissleder R, Papisov M, Bogdanov A Jr, Brady TJ. Monocrystalline iron oxide nanocompounds (MION): physicochemical properties. Magn Reson Med 1993;29:599–604.

20. Wunderbaldinger P, Josephson L, Weissleder R. Tat peptide directs enhanced clearance and hepatic permeability of magnetic nanoparticles. Bioconjug Chem 2002;13:264–268.

21. Choi SH, Han MH, Moon WK, et al. Cervical lymph node metastases: MR imaging of gadofluorine M and monocrystalline iron oxide nanoparticle-47 in a rabbit model of head and neck cancer. Radiology 2006;241:753–762.

22. Schar M, Kozerke S, Fischer SE, Boesiger P. Cardiac SSFP imaging at 3 Tesla. Magn Reson Med 2004;51:799–806.

23. Crawley AP, Henkelman RM. A comparison of one-shot and recovery methods in T1 imaging. Magn Reson Med 1988;7:23–34.

24. Fleckenstein JL, Archer BT, Barker BA, Vaughan JT, Parkey RW, Peshock RM. Fast short-tau inversion-recovery MR imaging. Radiology 1991;179:499–504.

25. Etienne A, Botnar RM, Van Muiswinkel AM, Boesiger P, Manning WJ, Stuber M. "Soap-bubble" visualization and quantitative analysis of 3D coronary magnetic resonance angiograms. Magn Reson Med 2002;48:658–666.

26. Korosoglou G, Gilson WD, Schar M, et al. Hind limb ischemia in rabbit model: T2-prepared versus time-of-flight MR angiography at 3 T. Radiology 2007;245:761–769.

27. Anzai Y, Piccoli CW, Outwater EK, et al. Evaluation of neck and body metastases to nodes with ferumoxtran 10-enhanced MR imaging: phase III safety and efficacy study. Radiology 2003;228:777–788.

28. Harisinghani MG, Barentsz J, Hahn PF, et al. Noninvasive detection of clinically occult lymph-node metastases in prostate cancer. N Engl J Med 2003;348:2491–2499.

29. Ruehm SG, Corot C, Vogt P, Kolb S, Debatin JF. Magnetic resonance imaging of atherosclerotic plaque with ultrasmall superparamagnetic particles of iron oxide in hyperlipidemic rabbits. Circulation 2001;103:415–422.

30. Kooi ME, Cappendijk VC, Cleutjens KB, et al. Accumulation of ultrasmall superparamagnetic particles of iron oxide in human atherosclerotic plaques can be detected by in vivo magnetic resonance imaging. Circulation 2003;107:2453–2458.

31. Kodama T, Watanabe K. Influence of imaging parameters, flow velocity, and pulsatile flow on three-dimensional time-of-flight MR angiography: experimental studies. Eur J Radiol 1997;26:83–91.

32. Bourrinet P, Bengele HH, Bonnemain B, et al. Preclinical safety and pharmacokinetic profile of ferumoxtran-10, an ultrasmall superparamagnetic iron oxide magnetic resonance contrast agent. Invest Radiol 2006; 41:313–324.

Radiology 2008

This is your reprint order form or pro forma invoice

(Please keep a copy of this document for your records.)

Reprint order forms and purchase orders or prepayments must be received 72 hours after receipt of form either by mail or by fax at 410-820-9765. It is the policy of Cadmus Reprints to issue one invoice per order. **Please print clearly**.

Author Name _____
Title of Article _____
Issue of Journal_____ Reprint # _____ Publication Date _____
Number of Pages_____ KB # _____ Symbol Radiology
Color in Article? Yes / No (Please Circle)

Please include the journal name and reprint number or manuscript number on your purchase order or other correspondence.

Order and Shipping Information

Reprint Costs **(Please see page 2 of 2 for reprint costs/fees.)**

_____ Number of reprints ordered $_____
_____ Number of color reprints ordered $_____
_____ Number of covers ordered $_____
Subtotal $_____
Taxes $_____

(*Add appropriate sales tax for Virginia, Maryland, Pennsylvania, and the District of Columbia or Canadian GST to the reprints if your order is to be shipped to these locations*.)

First address included, add $32 for each additional shipping address $_____

TOTAL $_____

Shipping Address **(cannot ship to a P.O. Box) Please Print Clearly**

Name _____
Institution _____
Street _____
City _____ State _____ Zip _____
Country _____
Quantity_____ Fax _____
Phone: Day _____ Evening _____
E-mail Address _____

Additional Shipping Address* **(cannot ship to a P.O. Box)**

Name _____
Institution _____
Street _____
City _____ State _____ Zip _____
Country _____
Quantity _____ Fax _____
Phone: Day _____ Evening _____
E-mail Address _____
** Add $32 for each additional shipping address*

Payment and Credit Card Details

Enclosed: Personal Check _____
Credit Card Payment Details _____
Checks must be paid in U.S. dollars and drawn on a U.S. Bank.

Credit Card: __ VISA __ Am. Exp. __ MasterCard
Card Number _____
Expiration Date_____
Signature: _____

Please send your order form and prepayment made payable to:

Cadmus Reprints
P.O. Box 751903
Charlotte, NC 28275-1903

Note: Do not send express packages to this location, PO Box.
FEIN #:541274108

Invoice or Credit Card Information

Invoice Address Please Print Clearly
Please complete Invoice address as it appears on credit card statement

Name _____
Institution _____
Department _____
Street _____
City _____ State _____ Zip _____
Country _____
Phone _____ Fax _____
E-mail Address _____

Cadmus will process credit cards and *Cadmus Journal Services* will appear on the credit card statement.

If you don't mail your order form, you may fax it to 410-820-9765 with your credit card information.

Signature _____ Date _____
Signature is required. By signing this form, the author agrees to accept the responsibility for the payment of reprints and/or all charges described in this document.

RB-9/26/07

Radiology 2008

Black and White Reprint Prices

Domestic (USA only)						
# of Pages	50	100	200	300	400	500
1-4	$221	$233	$268	$285	$303	$323
5-8	$355	$382	$432	$466	$510	$544
9-12	$466	$513	$595	$652	$714	$775
13-16	$576	$640	$749	$830	$912	$995
17-20	$694	$775	$906	$1,017	$1,117	$1,220
21-24	$809	$906	$1,071	$1,200	$1,321	$1,471
25-28	$928	$1,041	$1,242	$1,390	$1,544	$1,688
29-32	$1,042	$1,178	$1,403	$1,568	$1,751	$1,924
Covers	$97	$118	$215	$323	$442	$555

International (includes Canada and Mexico)						
# of Pages	50	100	200	300	400	500
1-4	$272	$283	$340	$397	$446	$506
5-8	$428	$455	$576	$675	$784	$884
9-12	$580	$626	$805	$964	$1,115	$1,278
13-16	$724	$786	$1,023	$1,232	$1,445	$1,652
17-20	$878	$958	$1,246	$1,520	$1,774	$2,030
21-24	$1,022	$1,119	$1,474	$1,795	$2,108	$2,426
25-28	$1,176	$1,291	$1,700	$2,070	$2,450	$2,813
29-32	$1,316	$1,452	$1,936	$2,355	$2,784	$3,209
Covers	$156	$176	$335	$525	$716	$905

Color Reprint Prices

Domestic (USA only)						
# of Pages	50	100	200	300	400	500
1-4	$223	$239	$352	$473	$597	$719
5-8	$349	$401	$601	$849	$1,099	$1,349
9-12	$486	$517	$852	$1,232	$1,609	$1,992
13-16	$615	$651	$1,105	$1,609	$2,117	$2,624
17-20	$759	$787	$1,357	$1,997	$2,626	$3,260
21-24	$897	$924	$1,611	$2,376	$3,135	$3,905
25-28	$1,033	$1,071	$1,873	$2,757	$3,650	$4,536
29-32	$1,175	$1,208	$2,122	$3,138	$4,162	$5,180
Covers	$97	$118	$215	$323	$442	$555

International (includes Canada and Mexico))						
# of Pages	50	100	200	300	400	500
1-4	$278	$290	$424	$586	$741	$904
5-8	$429	$472	$746	$1,058	$1,374	$1,690
9-12	$604	$629	$1,061	$1,545	$2,011	$2,494
13-16	$766	$797	$1,378	$2,013	$2,647	$3,280
17-20	$945	$972	$1,698	$2,499	$3,282	$4,069
21-24	$1,110	$1,139	$2,015	$2,970	$3,921	$4,873
25-28	$1,290	$1,321	$2,333	$3,437	$4,556	$5,661
29-32	$1,455	$1,482	$2,652	$3,924	$5,193	$6,462
Covers	$156	$176	$335	$525	$716	$905

Minimum order is 50 copies. For orders larger than 500 copies, please consult Cadmus Reprints at 800-407-9190.

Reprint Cover

Cover prices are listed above. The cover will include the publication title, article title, and author name in black.

Shipping

Shipping costs are included in the reprint prices. Domestic orders are shipped via UPS Ground service. Foreign orders are shipped via a proof of delivery air service.

Multiple Shipments

Orders can be shipped to more than one location. Please be aware that it will cost $32 for each additional location.

Delivery

Your order will be shipped within 2 weeks of the journal print date. Allow extra time for delivery.

Tax Due

Residents of Virginia, Maryland, Pennsylvania, and the District of Columbia are required to add the appropriate sales tax to each reprint order. For orders shipped to Canada, please add 7% Canadian GST unless exemption is claimed.

Ordering

Reprint order forms and purchase order or prepayment is required to process your order. Please reference journal name and reprint number or manuscript number on any correspondence. You may use the reverse side of this form as a proforma invoice. Please return your order form and prepayment to:

Cadmus Reprints
P.O. Box 751903
Charlotte, NC 28275-1903

Note: Do not send express packages to this location, PO Box.
FEIN #:541274108

Please direct all inquiries to:

Rose A. Baynard
800-407-9190 (toll free number)
410-819-3966 (direct number)
410-820-9765 (FAX number)
baynardr@cadmus.com (e-mail)

Reprint Order Forms and purchase order or prepayments must be received 72 hours after receipt of form.